Creation of metasurface from vertically aligned carbon nanotubes as versatile platform for ultra-light THz components

G.V. Gorokhov[1,2], D.S. Bychanok[1,3], P.P. Kuzhir[1,4], D.V. Gorodetskiy[5], A.G. Kurenya[5], O.V. Sedelnikova[3,5], L.G. Bulusheva[3,5] and A.V. Okotrub[3,5]

[1]Institute for Nuclear Problems Belarusian State University, 11 Bobruiskaya str., 220030, Minsk, Belarus

[2]Physics Faculty, Vilnius University, Sauletekio 9, Vilnius LT-10222, Lithuania

[3]Tomsk State University, 36 Lenin Ave, Tomsk 634050, Russia

[4]Institute of Photonics, University of Eastern Finland, Yliopistokatu 7, FI-80101 Joensuu, Finland

[5]Nikolaev Institute of Inorganic Chemistry, SB RAS, 3 Acad. Lavrentiev Ave., 630090, Novosibirsk, Russia

E-mail: `glebgorokhov@yandex.ru`

November 2019

Abstract. Here a simple and reproducible method for obtaining terahertz metasurfaces formed from multiwall carbon nanotubes (MWCNTs) is presented. The metasurfaces were obtained from a vertically aligned array of MWCNTs using a laser engraving technique followed by polymer covering. The structures under study demonstrate frequency-selective reflection in terahertz range following the Huygens–Fresnel formalism. For a normal incidence of the electromagnetic wave, the model for numerical calculation of backscattering from the metasurfaces was proposed. Lightweight and compact MWCNT-based metasurfaces are capable to replace conventional pyramidal absorbers and proved to serve as a versatile platform for scalable cost-efficient production of ultra-light electromagnetic components for THz applications.

Keywords: Terahertz absorption, carbon nanotubes, diffraction gratings, periodic structures

Submitted to: *Nanotechnology*

1. Introduction

Carbon nanotubes (CNTs) are well-known as perfect filler [1, 2, 3, 4, 5, 6] and even the substrate [7] for producing lightweight composites for electromagnetic applications. Along with graphene [8] the unique properties of CNTs allow creating compact durable and/or flexible [9] electromagnetic components and nano-devices, such as antennas [10, 11, 12], interconnects [13, 14], polarizers [15, 16], sensors [17], detectors (see [18] and Refs therein) and emitters of sub-mm waves radiation (see [19] and Refs).

Such a wide applicability of CNTs is due to their unique electromagnetics arising from plasmon-polariton (i.e. slowed-down surface wave) propagating along CNT axis [20], as well as so-called finite length effects (i.e. localized plasmon resonance) inherent for micron-length single-walled nanotube at THz and far-infrared frequencies [21, 22]. The valuable skin effect caused by electromagnetic radiation screening in low frequency ranges [23, 24] up to microwaves was predicted and experimentally observed for long multi-walled carbon nanotubes (MWCNTs). The recently demonstrated negative photo-induced conductivity [25] supported the possibility of ultra-fast tuning of CNTs THz optical density that opens an opportunity for the development of electromagnetic devices. To summarize, percolated composites [4, 6, 26], films [1, 17], meshes and sponges [27] behave like ultra-lightweight quasi-metals, demonstrating conductivity peaks at THz range in case of relatively short single-walled CNTs. In case of long single-walled [28] and multi-walled CNTs, and CNT bundles [29] the conductivity peak shifts towards much lower frequencies (hundreds of MHz and GHz).

However, in many cases, when individual CNT's characteristic parameters are not compatible with the wavelength taking into account slowing down effect, one may consider CNT array, film or composite as a macroscopic homogenized structure, which electromagnetic response is governed by averaged conductivity, rather than fundamental electromagnetics specific to individual CNTs. In such case one typically has porous conductive structure with broadband absorption [27], which properties are dependent on the CNT array/film density, conductivity and geometry of single tubes forming the array, inter-tubes contact resistance, etc. In order to effectively reach the electromagnetic properties required by a particular application the metamaterial paradigm [30, 31, 32, 33] can be applied to the CNT array combining its intrinsic properties with particular patterning providing the constructive interference [34].

The idea of this communication is to propose the versatile platform for scalable cost-efficient production of ultra-light electromagnetic components based on patterned vertically aligned arrays of MWCNTs. We demonstrate that MWCNT arrays grown via conventional aerosol assisted synthesis may be easily machined using a laser engraving technique in order to obtain complex geometry structures. As a proof of concept, several 3D-metasurfaces made of pyramidal CNT arrays with pyramids height about $0.1-0.5$ mm (see Fig. 1) has been successfully produced and experimentally examined in $0.1-1$ THz frequency range. At the same time, the possibility of tuning the electromagnetic response of such material was studied theoretically in $0.01-10$ THz frequency range. The studied 3D CNT-based metasurface covered with a thin layer of insulating polymer is proved to be effective anti-reflection coating and reflection selective surface for THz range, supporting the ideology of scalable protocol of producing 3D metasurfaces composed of CNT-arrays as microwave-to-THz components.

The present paper is organized as follows. Section 2 contains the details of ordered MWCNT arrays preparation, structures engraving and experimental terahertz measurements. The basic principles of investigated structure electromagnetic response modeling are described at Section 3. Herein, the theoretical approach is compared with the experimental and absorption properties of the ordered CNT arrays are discussed. Finally, the Conclusions section summarizes the findings and gives an outlook on potential application of such metasurfaces.

2. Experimental

2.1. Preparation of materials

Vertically aligned MWCNT arrays were grown on silicon substrates using an aerosol-assisted CCVD method described elsewhere [35].

A silicon substrate was placed into the tubular oven constantly flowed with argon and heated at 800 °C. The synthesis was carried out using 2 % ferrocene ($Fe(C_5H_5)_2$) solution in toluene ($C_6H_5CH_3$). As a result, with the use of 2.5 ml of the reaction mixture an aligned MWCNT array of $\sim 250\ \mu$m height was obtained. To examine the morphology of MWCNTs, the pristine sample was investigated by transmission electron microscopy (TEM) using a JEOL 2010 microscope. TEM image of obtained MWCNTs is shown at Fig. 1 (a). Average diameter of nanotubes is ~ 6 nm.

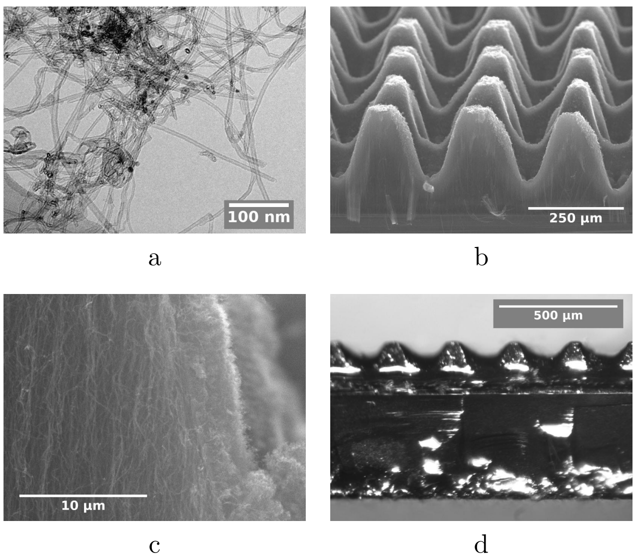

Figure 1. (a) TEM image of MWCNTs obtained by CVD technology; (b, c) SEM images of MWCNT-based pyramids periodic array ; (d) Image of the general view of arrays covered with epoxy layer.

The plane-parallel MWCNT arrays were transformed to the arrays of pyramids using laser engraving. The industrial laser engraver (Winseal, China) with 20 Wt CO_2 laser and 20 mm/s scanning speed was used. Grating period was 250 μm. To study the structure of the engraved sample and to prove the preservation of nanotubes after the laser treatment, the obtained sample was investigated by scanning electron microscopy (SEM) using a JEOL JSM 6700F microscope. The SEM images of engraved pyramids are presented in Fig. 1 (b, c).

After the engraving array of pyramids was covered with epoxy resin in order to protect its fragile structure. The viscous epoxy resin (Crystal 76) was dropped and then spread over the engraved surface under the vacuum. Total height of pyramids after all manipulations measured by means of optic microscopy was $232.9 \pm 11.9\ \mu$m with $54.9 \pm 6.9\ \mu$m uncut layer at the bottom. General view of structures after covering with the epoxy resin is presented in Fig. 1 (d). The impact to electromagnetic response of the investigated system done by polymer cover is discussed in the section 3.

2.2. Terahertz measurements

The THz measurements were carried out using a commercial THz time domain spectrometer "TSPEC" by EKSPLA in 0.1 – 1.0 THz frequency range. The sample was placed normally to the initial electromagnetic wave. According to its functioning principle, the THz spectrometer registers the waveform of THz electrical field with perfect reflector (as a reference) and with sample (as experimental data). For the purpose to increase signal-to-noise ratio each measurement is averaged over 1024 frames. In order to switch between time and frequency domains the Fourier transform is used. The reflection coefficient is evaluated as a ratio between powers of electromagnetic radiation reflected by the sample and the reference.

3. Modeling

3.1. Periodic structure contribution

Let us consider the backscattering of plane wave from the infinite array of conductive square pyramids with height h and base width l (see Fig. 2).

There are several approaches to calculate the amplitude of the signal reflected by such a structure. In the low frequency region the wavelength is much higher than the characteristic lateral size of pyramids that allows to implement the long-wave approximation and homogenization [36, 37]. When the wavelength is substantially smaller with respect to the characteristic lateral size of pyramids, the electromagnetic response obeys the principles of linear optics [38]. However, when the wavelength and characteristic dimensions of system are comparable, the Huygens–Fresnel principle should be applied for waves scattering calculations.

Let us consider the wave with amplitude E_0, which is propagated normally to pyramids bases (along the X axis, Figure 2 a) and reflected back. According to the Huygens–Fresnel principle, each point of a wavefront acts as a source of secondary waves, which interfering with each other determine total wavefront. In order to recreate the wavefront of pyramidal array let us consider one edge of a single pyramid (for example edge 1 in Fig. 2 (b)). The scattering conditions from all points of the edge are the same except of the path difference, which is equal to $\Delta_x = 2x$ for normal backscattering. Here, only the tangential component $E_0 \cos \Theta$ should be considered because the contribution of normal component (E_n in Fig. 2 (b)) from equivalent places of edges 1 and 3 are in antiphase.

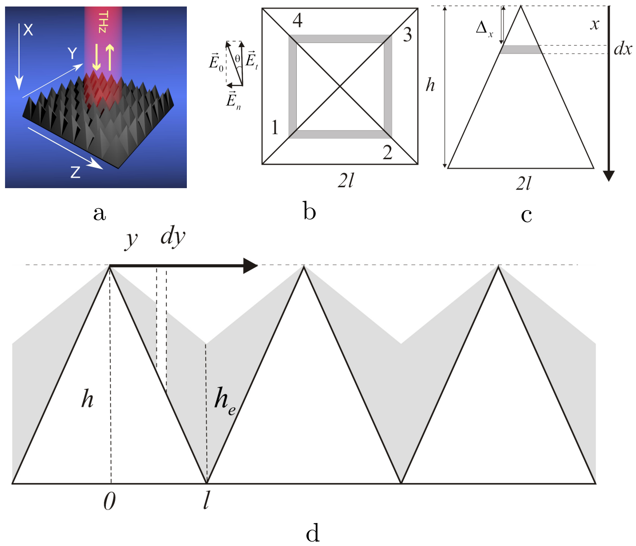

Figure 2. Backscattering of plane wave from pyramidal array. (a) Pyramidal array reflecting the terahertz radiation, (b) top view, (c) side view, (d) schematic image of pyramidal array covered with dielectric polymer.

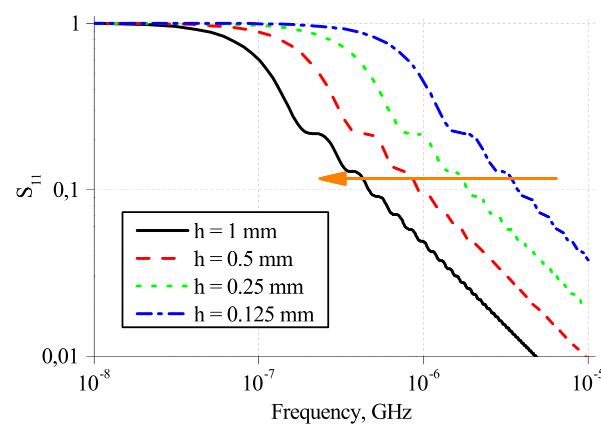

Figure 3. The frequency dependence of S_{11} on pyramid height $h = 0.125$, 0.25, 0.5, 1.0 mm.

The contribution of dx-thick layer of edge 1 placed on distance x from the top of pyramid to the total reflected amplitude is:

$$dE_{t1} = \frac{E_0 \cos\Theta \exp(i\omega t - ik\Delta_x)}{S_{edge}} dS = \tag{1}$$
$$= \frac{E_0 \cos\Theta \exp(i\omega t - ik2x)}{h^2} 2x dx,$$

where k is the wave vector, h is the height of pyramid.

The total contribution of the edge 1 is:

$$E_{t1} = \frac{E_0 \cos\Theta \exp(i\omega t)}{h^2} \int_0^h 2x \exp(-ik2x) dx = \tag{2}$$
$$= \frac{E_0 \cos\Theta \exp(i\omega t)}{2k^2h^2} \left[\exp[-i2kh](1+2ikh) - 1\right].$$

The contribution of the edge 3 is the same as Eq. (2). Contributions of the edges 2 and 4 may be obtained from Eq. (2) by substitution of $\cos\Theta$ for $\sin\Theta$.

Summarizing the impact of all four edges, it is possible to obtain the scattering parameter S_{11}^p (ratio between reflected and incident radiation amplitudes) for the surface paved with pyramids:

$$S_{11}^p(\nu, h) = \frac{(1+2ikh)\exp[-i2kh] - 1}{2k^2h^2}. \tag{3}$$

In Fig. 3 the S_{11}^p frequency dependence is presented for various h. Here, the pyramids consist of perfect electric conductor i.e. the flat surface of such material has $|S_{11}|$=1.

The increase of pyramid height h shifts the S_{11}^p spectrum to the low frequency region. Fig. 3 clearly depicts the transition between long-wave approximation through the Huygens–Fresnel theory to the geometric optics region. At low frequencies the wavelength is much higher than the pyramid height h, thus the structure interacts with radiation as a perfect reflector. When the wavelength is comparable with h, the amplitude of back-reflected signal decreased with relatively small oscillations caused by interference. Finally, at high frequencies, the S_{11}^p value is significantly damped and back-reflection becomes negligible.

3.2. Dielectric Layer contribution

A widely known example of matching layer is the optical lens antireflective coating, which decreases the difference between refractive indices of free space and lens making their interface less reflective. For the pyramids array covered with dielectric layer the amplitude of back-reflected signal is also dependent on the dielectric permittivity ε and thickness τ of the latter. To calculate dielectric layer contribution it is necessary to take into account the interference between waves reflecting from top and bottom surfaces of dielectric layer covering the pyramids. The electric field E_I in the region above dielectric layer (in free space) and electric field E_{II} inside the layer may be determined as:

$$E_I = C_1 \exp[-ik_1x] + C_2 \exp[ik_1x] \tag{4}$$
$$E_{II} = C_3 \exp[-ik_2x] + C_3\alpha \exp[ik_2x],$$

where C_1, C_2, C_3 are unknown coefficients, $k_1 = \frac{2\pi\nu}{c}$ and $k_2 = \frac{2\pi\nu\sqrt{\varepsilon}}{c}$ are wavenumbers in the free space and in the dielectric layer respectively, ν is the frequency, c is the speed of light. The amplitudes of initial and reflected waved were taken to be C_3 and αC_3 respectively. A term ($|\alpha| \leq 1$) implies imperfection of CNT array as conductor. Therefore, α may be considered as amplitude of the signal reflected by a plane surface of conductive material with semi-infinite depth (in considered case, the CNT array) into a medium (polymer) with the dielectric constant ε. Eq. (4) should satisfy the following boundary conditions:

$$E_I(-\tau) = E_{II}(-\tau), \qquad (5)$$
$$\frac{\partial E_I}{\partial x}|_{-\tau} = \frac{\partial E_{II}}{\partial x}|_{-\tau}.$$

Solving Eq. (4)-(5) allows to obtain the amplitude of reflected signal from the plane-parallel layer of dielectric with non-perfect back reflector:

$$S_{11}^d(\nu,\tau,\varepsilon,\beta) = \frac{C_2}{C_1} = \qquad (6)$$
$$= \frac{e^{2i\tau k_1}\left(e^{2i\tau k_2}k_1 - e^{2i\tau k_2}k_2 + k_1\alpha + k_2\alpha\right)}{e^{2i\tau k_2}k_1 + e^{2i\tau k_2}k_2 + k_1\alpha - k_2\alpha}.$$

Eq. (6) describes the contribution of dielectric layer to the reflection coefficient of epoxy covered pyramidal CNT array. The parameter $\alpha = \frac{\sqrt{(\varepsilon)}-(1-\beta)/(1+\beta)}{\sqrt{(\varepsilon)}+(1-\beta)/(1+\beta)}$ is related to the amplitude of reflected signal $|\beta| \leq 1$ from plane back reflector in the free space. In the case when $\beta = -1$, Eq. (6) coincides with the amplitude of reflected signal from dielectric layer located on the perfect conductor [39] excepting the phase factor $\exp[2i\tau k_1]$. In order to represent the normal reflection of THz wave from plane-parallel MWCNT array $\beta = -0.9$ was used.

Fig. 4 shows the frequency dependence of S_{11} for the dielectric layer of $\tau = 0.1, 0.2, 0.3$ mm thickness.

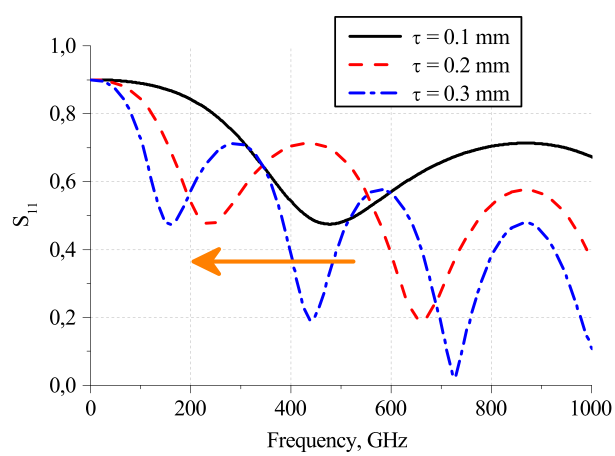

Figure 4. Frequency dispersion of S_{11} scattering parameter at different dielectric layer thickness $\tau = 0.1, 0.2, 0.3$ mm. ($\beta = -0.9$, $\varepsilon = 3 - 0.4i$)

The typical value for epoxy resin permittivity in THz frequency region $\varepsilon = 3 - 0.4i$ was used. Fig. 4 depicts the typical interference oscillations, which are absent for non-covered pyramids. When the dielectric layer becomes thickner, these oscillations shift to the low-frequency region.

3.3. Combination of dielectric layer and structure contribution

The real pyramidal array was impregnated with epoxy resin to overcome the pristine pyramids brittleness. The electromagnetic response of such structure is defined by both contributions from dielectric layer and from pyramidal back reflector. Due to surface tension forces, the epoxy resin unevenly covers the CNT pyramids array. As a first approximation, we considered the case when the thickness of the epoxy increases linearly with approaching the base of the pyramid (Fig. 2 (d))). In this case the amplitude of reflected signal from the unit cell may be calculated as:

$$S_{11} = \frac{2}{l^2}\int_0^l S_{11}^d(\nu, \frac{h_e}{l}x, \varepsilon, \beta) \times \qquad (7)$$
$$\exp[-i2k_1 x(\frac{h}{l} - \frac{h_e}{l})]x dx,$$

where l is the half length of pyramids base, h_e is the height of epoxy layer near the pyramids base. The first multiplier in Eq.(7) related to the dielectric layer contribution, the second - to the phase shift caused by the structure.

3.4. Comparison between experiment and modeling

The comparison between experimentally measured amplitude of the signal reflected by the array of pyramids covered with epoxy resin (Fig. 1 (d)) and fitted values obtained by Eq. (7) is presented in Fig. 5.

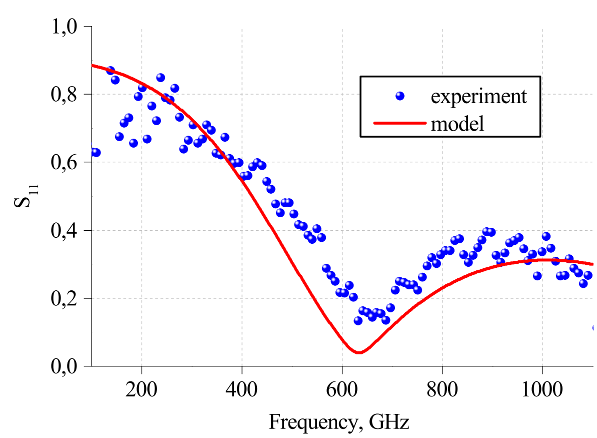

Figure 5. Amplitude of back-reflected signal S_{11} from periodic pyramidal CNT-array covered with epoxy resin layer (symbols correspond to the experimental data, line — to the modeling results).

The experimental data are in good agreement with modeling results. Mean absolute percentage error value was 6.4 %. The difference between experiment and modeling results may be related to the nonlinear dependence of epoxy layer thickness in the region near the pyramids base. The model curve in Fig. 5 was obtained with the following set of parameters: $\beta = -0.9$, $\varepsilon = 3 - 0.4i$, $h_e = 0.09$ mm, $h = 0.25$ mm. The results showed that the produced metasurface acts as reflection selective surface with maximal absorption near $\nu_0 = 700$ GHz. Below ν_0 the amplitude of signal reflected from CNT array is 0.8, while above ν_0 the S_{11} amplitude is near 0.4.

Conclusions

The concept of frequency selective reflector based on pyramidal metasurfaces was implemented and investigated. The impact of pyramids height and dielectric covering layer to the electromagnetic response of investigated structures was theoretically described in a wide frequency range. The possibility to control the reflective behavior of the metasurfaces was theoretically substantiated.

The metasurface was produced by the laser engraving of vertically aligned MWCNT array followed by the dielectric layer covering. In accordance with the theoretical prediction, the experimental reflection spectrum exhibited the local minima in the THz range. Its position is determined by the thickness of the dielectric cover, while the height of pyramids defines the dumping rate of the reflected signal.

The presented design of metasurfaces which effectively absorb the electromagnetic radiation in the submillimeter frequency range is one of the numerous examples of THz component (such as frequency selective surfaces, filters, lenses, attenuators, etc.) that is possible to be realized using perfect absorption ability and electromagnetic response peculiarities of 3D-patterned CNT arrays. Targeting to the technology readiness level 3, these experimental observations supported by simple analytical model provide a solid laboratory-proved background for scalable cost-efficient technological protocol of ultra-lightweight THz components.

ACKNOWLEDGEMENTS

The work is supported by RFBR Grant number 19-33-50048, the Academy of Finland Flagship Programme, Photonics Research and Innovation (PREIN), decision 320166, H2020 RISE project 734164 Graphene 3D and Horizon 2020 RISE DiSeTCom project 823728. PK is supported by Horizon 2020 IF TURANDOT project 836816 and Grant of the President of the Republic of Belarus in science, education, health, culture in 2019. GG is supported by World Federation of Scientists project "Science and Technologies". All coauthors are thankful for support by Tomsk State University Competitiveness Improvement Program.

References

[1] A. V. Okotrub, V. V. Kubarev, M. A. Kanygin, O. V. Sedelnikova, and L. G. Bulusheva. Transmission of terahertz radiation by anisotropic MWCNT/polystyrene composite films. *physica status solidi (b)*, 248(11):2568–2571, November 2011.

[2] D Bychanok, P Angelova, A Paddubskaya, D Meisak, L Shashkova, M Demidenko, A Plyushch, E Ivanov, R Krastev, R Kotsilkova, F Y Ogrin, and P Kuzhir. Terahertz absorption in graphite nanoplatelets/polylactic acid composites. *Journal of Physics D: Applied Physics*, 51(14):145307, April 2018.

[3] Giovanni Spinelli, Patrizia Lamberti, Vincenzo Tucci, Radost Ivanova, Sonia Tabakova, Evgeni Ivanov, Rumiana Kotsilkova, Sossio Cimmino, Rosa Di Maio, and Clara Silvestre. Rheological and electrical behaviour of nanocarbon/poly(lactic)acid for 3d printing applications. *Composites Part B: Engineering*, 2018.

[4] Alfredo Ronca, Gennaro Rollo, Pierfrancesco Cerruti, Guoxia Fei, Xinpeng Gan, Giovanna Buonocore, Marino Lavorgna, Hesheng Xia, Clara Silvestre, and Luigi Ambrosio. Selective Laser Sintering Fabricated Thermoplastic Polyurethane/Graphene Cellular Structures with Tailorable Properties and High Strain Sensitivity. *Applied Sciences*, 9(5):864, February 2019.

[5] Mikhail Shuba, Dzmitry Yuko, Gleb Gorokhov, Darya Meisak, Dzmitry S Bychanok, Polina Kuzhir, Sergey A Maksimenko, Polya Angelova, Evgeni Ivanov, and Rumiana Kotsilkova. Frequency and density dependencies of the electromagnetic parameters of carbon nanotube and graphene nanoplatelet based composites in the microwave and terahertz ranges. *Materials Research Express*, July 2019.

[6] G. Gorokhov, D. Bychanok, D. Meisak, I. Shlyk, A. Liubimau, P. Angelova, C. Menseidov, E. Ivanov, R. Kotsilkova, M. Casa, P. Ciambelli, and P. Kuzhir. Carbon nanotubes vs graphene nanoplatelets for 3d-printable composites. *IOP Conference Series: Materials Science and Engineering*, 503:012010, March 2019.

[7] Junhong Chen and Ganhua Lu. Controlled decoration of carbon nanotubes with nanoparticles. *Nanotechnology*, 17(12):2891–2894, June 2006.

[8] A. K. Geim and K. S. Novoselov. The rise of graphene. In *Nanoscience and Technology*, pages 11–19. Co-Published with Macmillan Publishers Ltd, UK, August 2009.

[9] Yuto Kato, Masahiro Horibe, Seisuke Ata, Takeo Yamada, and Kenji Hata. Stretchable electromagnetic-interference shielding materials made of a long single-walled carbon-nanotube-elastomer composite. *RSC advances*, 7(18):10841–10847, 2017.

[10] G.W. Hanson. Fundamental transmitting properties of carbon nanotube antennas. *IEEE Transactions on Antennas and Propagation*, 53(11):3426–3435, November 2005.

[11] G. Ya Slepyan, M. V. Shuba, S. A. Maksimenko, and Akhlesh Lakhtakia. Theory of optical scattering by achiral carbon nanotubes and their potential as optical nanoantennas. *Physical Review B*, 73(19):195416, 2006.

[12] P.J. Burke, Shengdong Li, and Zhen Yu. Quantitative theory of nanowire and nanotube antenna performance. *IEEE Transactions On Nanotechnology*, 5(4):314–334, July 2006.

[13] Hong Li, Wen-Yan Yin, Kaustav Banerjee, and Jun-Fa Mao. Circuit Modeling and Performance Analysis of Multi-Walled Carbon Nanotube Interconnects. *IEEE*

Transactions on Electron Devices, 55(6):1328–1337, June 2008.

[14] A. Maffucci, G. Miano, and F. Villone. A New Circuit Model for Carbon Nanotube Interconnects With Diameter-Dependent Parameters. *IEEE Transactions on Nanotechnology*, 8(3):345–354, May 2009.

[15] D. S. Bychanok, M. V. Shuba, P. P. Kuzhir, S. A. Maksimenko, V. V. Kubarev, M. A. Kanygin, O. V. Sedelnikova, L. G. Bulusheva, and A. V. Okotrub. Anisotropic electromagnetic properties of polymer composites containing oriented multiwall carbon nanotubes in respect to terahertz polarizer applications. *Journal of Applied Physics*, 114(11):114304, September 2013.

[16] O V Sedelnikova, E Yu Korovin, K V Dorozhkin, M A Kanygin, V E Arkhipov, Yu V Shubin, V A Zhuravlev, V I Suslyaev, L G Bulusheva, and A V Okotrub. Iron-filled multi-walled carbon nanotubes for terahertz applications: effects of interfacial polarization, screening and anisotropy. *Nanotechnology*, 29(17):174003, April 2018.

[17] Prasad Dharap, Zhiling Li, Satish Nagarajaiah, and E V Barrera. Nanotube film based on single-wall carbon nanotubes for strain sensing. *Nanotechnology*, 15(3):379–382, March 2004.

[18] V. Ryzhii, T. Otsuji, M. Ryzhii, V. G. Leiman, G. Fedorov, G. N. Goltzman, I. A. Gayduchenko, N. Titova, D. Coquillat, D. But, W. Knap, V. Mitin, and M. S. Shur. Two-dimensional plasmons in lateral carbon nanotube network structures and their effect on the terahertz radiation detection. *Journal of Applied Physics*, 120(4):044501, July 2016.

[19] R R Hartmann, J Kono, and M E Portnoi. Terahertz science and technology of carbon nanomaterials. *Nanotechnology*, 25(32):322001, August 2014.

[20] G. Ya Slepyan, S. A. Maksimenko, Akhlesh Lakhtakia, O. Yevtushenko, and A. V. Gusakov. Electrodynamics of carbon nanotubes: Dynamic conductivity, impedance boundary conditions, and surface wave propagation. *Physical Review B*, 60(24):17136, 1999.

[21] G. Ya. Slepyan, M. V. Shuba, S. A. Maksimenko, C. Thomsen, and A. Lakhtakia. Terahertz conductivity peak in composite materials containing carbon nanotubes: Theory and interpretation of experiment. *Physical Review B*, 81(20), May 2010.

[22] M. V. Shuba, A. G. Paddubskaya, A. O. Plyushch, P. P. Kuzhir, G. Ya Slepyan, S. A. Maksimenko, V. K. Ksenevich, P. Buka, D. Seliuta, and I. Kasalynas. Experimental evidence of localized plasmon resonance in composite materials containing single-wall carbon nanotubes. *Physical Review B*, 85(16):165435, 2012.

[23] Mikhail V. Shuba, Gregory Ya. Slepyan, Sergey A. Maksimenko, and George W. Hanson. Radiofrequency field absorption by carbon nanotubes embedded in a conductive host. *Journal of Applied Physics*, 108(11):114302, December 2010.

[24] M. V. Shuba, A. V. Melnikov, A. G. Paddubskaya, P. P. Kuzhir, S. A. Maksimenko, and C. Thomsen. Role of finite-size effects in the microwave and subterahertz electromagnetic response of a multiwall carbon-nanotube-based composite: Theory and interpretation of experiments. *Physical Review B*, 88(4):045436, 2013.

[25] Peter Karlsen, Mikhail V. Shuba, Polina P. Kuzhir, Albert G. Nasibulin, Patrizia Lamberti, and Euan Hendry. Sign inversion in the terahertz photoconductivity of single-walled carbon nanotube films. *Physical Review B*, 98(24):241404, 2018.

[26] O.V. Sedelnikova, M.A. Kanygin, E.Yu. Korovin, L.G. Bulusheva, V.I. Suslyaev, and A.V. Okotrub. Effect of fabrication method on the structure and electromagnetic response of carbon nanotube/polystyrene composites in low-frequency and Ka bands. *Composites Science and Technology*, 102:59–64, October 2014.

[27] M V Shuba, D I Yuko, P P Kuzhir, S A Maksimenko, M De Crescenzi, and M Scarselli. Carbon nanotube sponges as tunable materials for electromagnetic applications. *Nanotechnology*, 29(37):375202, September 2018.

[28] B.P. Gorshunov, E.S. Zhukova, Ju.S. Starovatykh, M.A. Belyanchikov, A.K. Grebenko, A.V. Bubis, V.I. Tsebro, A.A. Tonkikh, D.V. Rybkovskiy, A.G. Nasibulin, E.I. Kauppinen, and E.D. Obraztsova. Terahertz spectroscopy of charge transport in films of pristine and doped single-wall carbon nanotubes. *Carbon*, 126:544–551, January 2018.

[29] Polina P. Kuzhir, Alesia G. Paddubskaya, Mikhail V. Shuba, Sergey A. Maksimenko, Alain Celzard, Vanessa Fierro, Gisele Amaral-Labat, Antonio Pizzi, Gintaras Valuis, Jan Macutkevic, Maksim Ivanov, Juras Banys, Silvia Bistarelli, Antonino Cataldo, Matteo Mastrucci, Federico Micciulla, Immacolata Sacco, Eleonora Stefanutti, and Stefano Bellucci. Electromagnetic shielding efficiency in Ka-band: carbon foam versus epoxy/carbon nanotube composites. *Journal of Nanophotonics*, 6(1):061715, December 2012.

[30] Shobhit K Patel, Mayurkumar Ladumor, Vishal Sorathiya, and Tianjing Guo. Graphene based tunable grating structure. *Materials Research Express*, 6(2):025602, November 2018.

[31] Shobhit K. Patel, Mayurkumar Ladumor, Juveriya Parmar, and Tianjing Guo. Graphene-based tunable reflector superstructure grating. *Applied Physics A*, 125(8), August 2019.

[32] Vladislav Popov, Marina Yakovleva, Fabrice Boust, Jean-Luc Pelouard, Fabrice Pardo, and Shah Nawaz Burokur. Designing Metagratings via Local Periodic Approximation: From Microwaves to Infrared. *Physical Review Applied*, 11(4), April 2019.

[33] Rajendrasinh Jadeja, Shreyas Charola, Shobhit K. Patel, Juveriya Parmar, Mayurkumar Ladumor, Truong Khang Nguyen, and Vigneswaran Dhasarathan. Numerical investigation of graphene-based efficient and broadband metasurface for terahertz solar absorber. *Journal of Materials Science*, 55(8):3462–3469, March 2020.

[34] Alesia Paddubskaya, Marina Demidenko, Konstantin Batrakov, Gintaras Valuis, Tommi Kaplas, Yuri Svirko, and Polina Kuzhir. Tunable Perfect THz Absorber Based on a Stretchable Ultrathin Carbon-Polymer Bilayer. *Materials*, 12(1):143, January 2019.

[35] A. V. Okotrub, L. G. Bulusheva, A. G. Kudashov, V. V. Belavin, and S. V. Komogortsev. Arrays of carbon nanotubes aligned perpendicular to the substrate surface: Anisotropy of structure and properties. *Nanotechnologies in Russia*, 3(3-4):191–200, 2008.

[36] D. S. Bychanok, A. O. Plyushch, G. V. Gorokhov, U. S. Bychanok, P. P. Kuzhir, and S. A. Maksimenko. Microwave radiation absorbers based on corrugated composites with carbon fibers. *Technical Physics*, 61(12):1880–1884, December 2016.

[37] D. Bychanok, Sijin Li, A. Sanchez-Sanchez, G. Gorokhov, P. Kuzhir, F. Y. Ogrin, Andreea Pasc, T. Ballweg, K. Mandel, and A. Szczurek. Hollow carbon spheres in microwaves: Bio inspired absorbing coating. *Applied Physics Letters*, 108(1):013701, 2016.

[38] Max Born and Emil Wolf. *Principles of optics: electromagnetic theory of propagation, interference and diffraction of light.* Cambridge University Press, Cambridge ; New York, 7th expanded ed edition, 1999.

[39] Dzmitry Bychanok, Gleb Gorokhov, Darya Meisak, Artyom Plyushch, Polina Kuzhir, Alexey Sokal, Konstantin Lapko, Angela Sanchez-Sanchez, Vanessa Fierro, and Alain Celzard. Exploring carbon nan-

otubes/BaTiO3/Fe3o4 nanocomposites as microwave absorbers. *Progress In Electromagnetics Research C*, 2016.

[40] Pawel Kopyt, Bartlomiej Salski, Przemyslaw Zagrajek, Daniel Janczak, Marcin Sloma, Malgorzata Jakubowska, Marzena Olszewska-Placha, and Wojciech Gwarek. Electric Properties of Graphene-Based Conductive Layers from DC Up To Terahertz Range. *IEEE Transactions on Terahertz Science and Technology*, 6(3):480–490, May 2016.

[41] Ying Lan, Baoqing Zeng, Hai Zhang, Beiran Chen, and Zhonghai Yang. SIMULATION OF CARBON NANOTUBE THz ANTENNA ARRAYS. *International Journal of Infrared and Millimeter Waves*, 27(6):871–877, February 2007.

[42] John F. O Hara, R. D. Averitt, and A. J. Taylor. Terahertz surface plasmon polariton coupling on metallic gratings. *Optics express*, 12(25):6397–6402, 2004.

[43] A. Szczurek, A. Ortona, L. Ferrari, E. Rezaei, G. Medjahdi, V. Fierro, D. Bychanok, P. Kuzhir, and A. Celzard. Carbon periodic cellular architectures. *Carbon*, 88:70–85, July 2015.

[44] Constantin R. Simovski, Pavel A. Belov, Alexander V. Atrashchenko, and Yuri S. Kivshar. Wire Metamaterials: Physics and Applications. *Advanced Materials*, 24(31):4229–4248, August 2012.

[45] Itsunari Yamada, Keisuke Takano, Masanori Hangyo, Mitsunori Saito, and Wataru Watanabe. Terahertz wire-grid polarizers with micrometer-pitch Al gratings. *Optics letters*, 34(3):274–276, 2009.

[46] G. A. Wurtz, R. Pollard, W. Hendren, G. P. Wiederrecht, D. J. Gosztola, V. A. Podolskiy, and A. V. Zayats. Designed ultrafast optical nonlinearity in a plasmonic nanorod metamaterial enhanced by nonlocality. *Nature Nanotechnology*, 6(2):107–111, February 2011.

[47] F. Qin and Christian Brosseau. A review and analysis of microwave absorption in polymer composites filled with carbonaceous particles. *Journal of applied physics*, 111(6):4, 2012.

[48] H. O. Moser, B. D. F. Casse, O. Wilhelmi, and B. T. Saw. Terahertz response of a microfabricated rod-split-ring-resonator electromagnetic metamaterial. *Physical review letters*, 94(6):063901, 2005.

[49] C. Castro, M. Pinault, S. Coste-Leconte, D. Porterat, Nedjma Bendiab, C. Reynaud, and M. Mayne-LHermite. Dynamics of catalyst particle formation and multi-walled carbon nanotube growth in aerosol-assisted catalytic chemical vapor deposition. *Carbon*, 48(13):3807–3816, 2010.

[50] M V Shuba, A G Paddubskaya, P P Kuzhir, S A Maksimenko, G Valusis, M Ivanov, J Banys, V Ksenevich, and G W Hanson. Observation of the microwave near-field enhancement effect in suspensions comprising single-walled carbon nanotubes. *Materials Research Express*, 4(7):075033, July 2017.

[51] Dmitri A. Tsyboulski, Sergei M. Bachilo, and R. Bruce Weisman. Versatile Visualization of Individual Single-Walled Carbon Nanotubes with Near-Infrared Fluorescence Microscopy. *Nano Letters*, 5(5):975–979, May 2005.